BEAMLINES
X7B, X18B, X19A

PUBLICATION
F. Zhang, J.M. Raitano, C. Chen, J.C. Hanson, W. Caliebe, S. Khalid, and S. Chan, "Phase Stability in Ceria-Zirconia Binary Oxide (1-x)$CeO_{2-x}ZrO_2$ Nanoparticles: The Effect of Ce^{3+} Concentration and the Redox Envirnment," *J. of Appl. Phys.*, **99**, 0843131-0843138 (2006).

FUNDING
U.S. Department of Energy
National Science Foundation

FOR MORE INFORMATION
Siu-Wai Chan
Dept. of Applied Physics and Applied Mathematics
Columbia University
sc174@columbia.edu

PHASE STABILITY IN CERIA-ZIRCONIA BINARY OXIDE NANOPARTICLES

F. Zhang[1], C.-H. Chen[1], J.M. Raitano[1], R.D. Robinson[1], I.P. Herman[1], J.C. Hanson[2], W.A. Caliebe[2], S. Khalid[2], and S.-W. Chan[1]

[1]Department of Applied Physics and Applied Mathematics, Materials Research Science and Engineering Center, Columbia University; [2]Brookhaven National Laboratory

Cerium oxide has been widely investigated as a key component in catalysts and as an electrolyte for solid oxide fuel cells because of its ability to release or store oxygen when in its cubic fluorite structure. This property, which is the alleged source of the oxygen storage capacity (OSC) of ceria, is much enhanced by a large surface area and a small particle size. However, at high temperatures, ceria particles are coarsened, resulting in a smaller total surface area and a lower catalytic efficiency. Alloying with other metal oxides, particularly zirconia, can halt this coarsening process. However, the zirconia content for most effective catalysis will cause the binary oxide in micron-sized particles to contain a substantial amount of tetragonal phase that does not have the OSC properties, In our study, nanoparticles of ceria-zirconia were found to have a stable cubic fluorite phase despite what was predicted by the normal "bulk" phase diagram. Furthermore, we proved that a reducing environment stabilizes the cubic phase to 90% zirconia.

Cerium oxide in the cubic fluorite structure has been widely investigated because of its multiple applications, such as catalyst and electrolyte material of solid oxide fuel cells. In particular, the structural properties of binary oxide system of ceria and zirconia (CeO_2–ZrO_2) are extensively studied because it retains the superb redox and oxygen storage capacity (OSC) properties, and prevents thermal instability against coarsening of CeO_2. However, its various phases have not been discussed in detail, particularly with crystallite size. In this study, we aimed to investigate the structural properties of its nanoparticles for phase information. Specifically, we aimed to address two areas: First, we looked for methods that can stabilize the c' phase for a higher zirconia concentration to lessen particle coarsening. Second, we ascertained the extent to which particle size affects phase stability. This has a significant impact on catalysis.

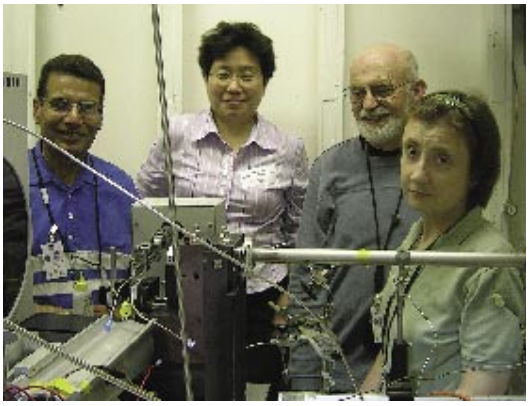

Authors (from left) Syed Khalid, Siu-Wai Chan, Jonathan C. Hanson, and Joan M. Raitano

Phase information of ceria–zirconia nanoparticles observed in air is studied by x-ray diffraction, transmission electron microscopy, and Raman spectroscopy. Particle size and composition are varied. Both the metastable tetragonal t' phase and the monoclinic m phase are not observed. The nanoscale of the particles likely stabilizes the tetragonal t phase against the formation of the monoclinic phase even at 100% zirconia. As the particle size decreases, both the c−t" and the c'−t phase boundaries shift to higher zirconia concentrations. The zirconia solubility limit increases with decreasing particle size such that the c and t" phases can be sustained at higher concentrations of zirconia before the corresponding formation of the t" and t phases. Raman scattering and XRD results are consistent in determining the emerging compositions of the t phase in the 1200° and the 800°C samples. The nanoparticles show different phases from those of the bulk in the CeO_2–ZrO_2 binary system. Nanoparticles of 20 nm and smaller having 35%–40% zirconia in ceria are 100% c' and stable against coarsening. The t" phase also likely contributes to OSC. This shows that the range of c' phase can be extended to high ZrO_2 concentrations by decreasing the c' crystallite size alone.

We observed that the range of the c' phase can extend to high ZrO_2 concentrations by decreasing the c' crystallite size alone. Earlier, we used x-ray absorption near edge spectroscopy (XANES) to demonstrate that the Ce^{3+} concentration in ceria nanoparticles increases with a decreasing crystallite size. Here, we investigated the valence state of Ce with varying ZrO_2 concentration and annealing atmosphere to better understand the phase stability in this nanocrystalline binary oxide system.

We used x-ray absorption near edge spectroscopy (XANES), time-resolved high temperature x-ray diffraction (XRD), and room temperature XRD to study the stability of the cubic phase (c') of $Ce_{1-x}Zr_xO_{2-y}$ nanoparticles. Results from XANES at the Ce L_{III} edge and the Zr L_{III} edge indicate the same phase transition point of c'-t for samples prepared in air. This is consistent with earlier results of XRD and Raman spectroscopy. The results show that the stability of the c' phase is directly related to the Ce^{3+} concentration. The percentage of the 3+ oxidation state of cerium was measured from the relative Ce^{3+} peak intensity at the Ce L_{III} edge in XANES. An 11% concentration of the larger Ce^{3+} ions, coupled with the smaller particle size, helps in releasing the local stress induced by the smaller Zr^{4+} ions and stabilizes the c' phase even under high zirconia concentrations of 40%–60%. XANES results at the Zr L_{III} edge supported the cubic phase stabilization. Under a reducing environment instead of in air, when the homogenization anneal was performed, the solubility limit of the cubic phase $Ce_{1-x}Zr_xO_{2-y}$ was extended to above 90% zirconia. The Ce^{3+} concentration increased, reaching 94% in $Ce_{0.1}Zr_{0.9}O_{2-y}$. Thus, the stability of c' phase is extended to higher ZrO_2 concentrations not by finer crystallite size alone but, more significantly, by a reducing environment.

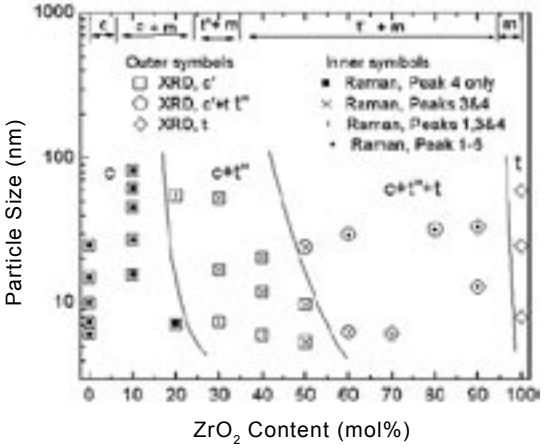

Figure 1. Phase stability diagram of $(1-x)CeO_{2-x}ZrO_2$ samples with various crystal size of the c' phase. There are overlapping symbols to denote XRD and Raman techniques in phase identification. Open symbols are from the XRD results and the inside symbols are from Raman scattering. Open squares (□): 100% c' phase present from XRD, circles (○): t phase present from XRD, diamonds (◊): only t phase present from XRD. Inner symbols, solid squares (■): only Raman peak 4 is present; vertical line (|): only Raman peaks 3 and 4 are present; crosses (×): only Raman peaks 1, 3 and 4 are present; dots (•): all Raman peaks 1-6 are present. At the top of the diagram are the phase fields identified at 800°C from reduced-quench-re-oxidized bulk/micron-size samples.

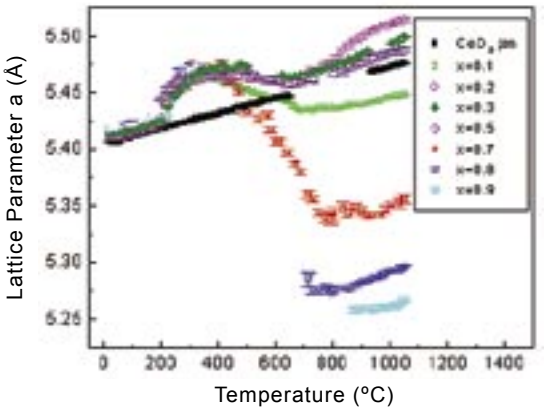

Figure 3. Lattice parameter study from in-situ XRD of as-prepared $(1-x)CeO_{2-x}ZrO_2$ in a reducing atmosphere as temperature increases. Each composition shown exhibits the cubic phase, c'.

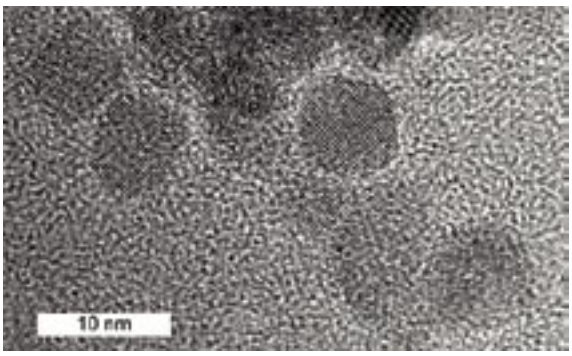

Figure 2. TEM lattice image of $Ce_{0.8}Zr_{0.2}O_{2-y}$ nanoparticles annealed previously at 900 °C.